Communication: Time-domain measurement of high-pressure N_2 and O_2 self-broadened linewidths using hybrid femtosecond/picosecond coherent anti-Stokes Raman scattering

Joseph D. Miller,[1] Sukesh Roy,[2] James R. Gord,[3] and Terrence R. Meyer[1,4,a)]
[1]*Department of Mechanical Engineering, Iowa State University, Ames, Iowa 50011, USA*
[2]*Spectral Energies, LLC, Dayton, Ohio 45431, USA*
[3]*Air Force Research Laboratory, Propulsion Directorate, Wright-Patterson Air Force Base, Ohio 45433, USA*
[4]*Erlangen Graduate School in Advanced Optical Technologies (SAOT), Friedrich-Alexander-University Erlangen-Nürnburg, Erlangen, Germany*

(Received 6 October 2011; accepted 15 November 2011; published online 28 November 2011)

The direct measurement of self-broadened linewidths using the time decay of pure-rotational hybrid femtosecond/picosecond coherent anti-Stokes Raman scattering (fs/ps RCARS) signals is demonstrated in gas-phase N_2 and O_2 from 1–20 atm. Using fs pump and Stokes pulses and a spectrally narrowed ps probe pulse, collisional dephasing rates with time constants as short as 2.5 ps are captured with high accuracy for individual rotational transitions. S-branch linewidths of N_2 and O_2 from ~0.06 to 2.2 cm^{-1} and the line separation of O_2 triplet states are obtained from the measured dephasing rates and compared with high-resolution, frequency-domain measurements and S-branch approximations using the modified exponential gap model. The accuracy of the current measurements suggests that the fs/ps RCARS approach is well suited for tracking the collisional dynamics of gas-phase mixtures over a wide range of pressures. © *2011 American Institute of Physics*. [doi:10.1063/1.3665932]

The use of femtosecond (fs) and picosecond (ps) laser sources for gas-phase coherent anti-Stokes Raman scattering (CARS) thermometry has grown significantly in recent years due to the high peak powers of these laser sources and interest in resolving the time dynamics of the molecular response.[1] In fs CARS, the temporally short and spectrally broad (transform-limited) pump and Stokes pulses allow highly efficient, in-phase, and impulsive excitation of the entire rovibrational or pure-rotational manifold.[1–3] In this case, the molecular response is resolved in time using the spectrally integrated signal, but the dephasing rate of individual (*J*-level) transitions cannot be measured directly.[2,3] In ps CARS, the ability to measure short time decays is limited by relatively long pump, Stokes, and probe pulse widths (typically ~100 ps) and by the need to avoid nonresonant background by temporally separating the probe pulse from the pump and Stokes pulses.[4–6] For measurements of collisional dephasing rates, especially at high pressure, the ideal approach is to utilize broad (fs) pump and Stokes pulses and a spectrally narrowed (ps) probe pulse that can simultaneously isolate each molecular transition while still resolving short ~ps decay times.

Recently, the authors demonstrated a hybrid fs/ps CARS technique that uses 100-fs pump and Stokes pulses to impulsively excite vibrational or pure rotational transitions of a molecule and a spectrally narrowed, 1–10 ps probe pulse for frequency-domain thermometry.[7,8] A similar single-beam approach using a pulse-shaped 7-fs pulse to produce the pump, Stokes, and probe pulses via phase and polarization discrimination has been demonstrated, although the spectral resolution was limited to ~5 cm^{-1} by the spatial light modulator.[9] The hybrid fs/ps CARS approach offers the ability to temporally discriminate against nonresonant background, similar to either fs or ps CARS, but has the unique capability to resolve gas-phase rotational spectra within several hundred fs after Raman excitation.[10] These features are ideal for studying the time dynamics of individual rotational transitions at elevated pressure. Above 1 atm, the linewidths of N_2 and O_2 can be considered purely pressure broadened, and Doppler contributions to the linewidth can be neglected. Hence, detection of collisional decay rates for rotational transitions using fs/ps CARS allows for direct measurement of spectral linewidths.[7]

In this work, a time- and frequency-resolved fs/ps rotational CARS (RCARS) technique is used to accurately measure and report self-broadened S-branch linewidths of N_2 and O_2 from 1–20 atm. Few direct measurements of self-broadened S-branch linewidths are reported in the literature, and many ps and ns rotational CARS models rely on S-branch approximations from Q-branch data which can lead to errors at high pressure.[11,12] These measurements are critical for the determination of temperature and relative species concentrations in gas-phase media, especially at high pressure, because rotational-level and species-dependent collisional dephasing rates can alter the Raman spectra and lead to significant measurement errors.[4,6]

The hybrid fs/ps RCARS system has been described previously[7,8,10] and is summarized briefly in this communication. The pump and Stokes pulses were derived from the 100-fs output of a regeneratively amplified Ti:sapphire laser centered at ~790 nm. The energy of each pulse was 40 μJ

a)Author to whom correspondence should be addressed. Electronic mail: trm@iastate.edu.

 © 2011 American Institute of Physics

Author complimentary copy. Redistribution subject to AIP license or copyright, see http://jcp.aip.org/jcp/copyright.jsp

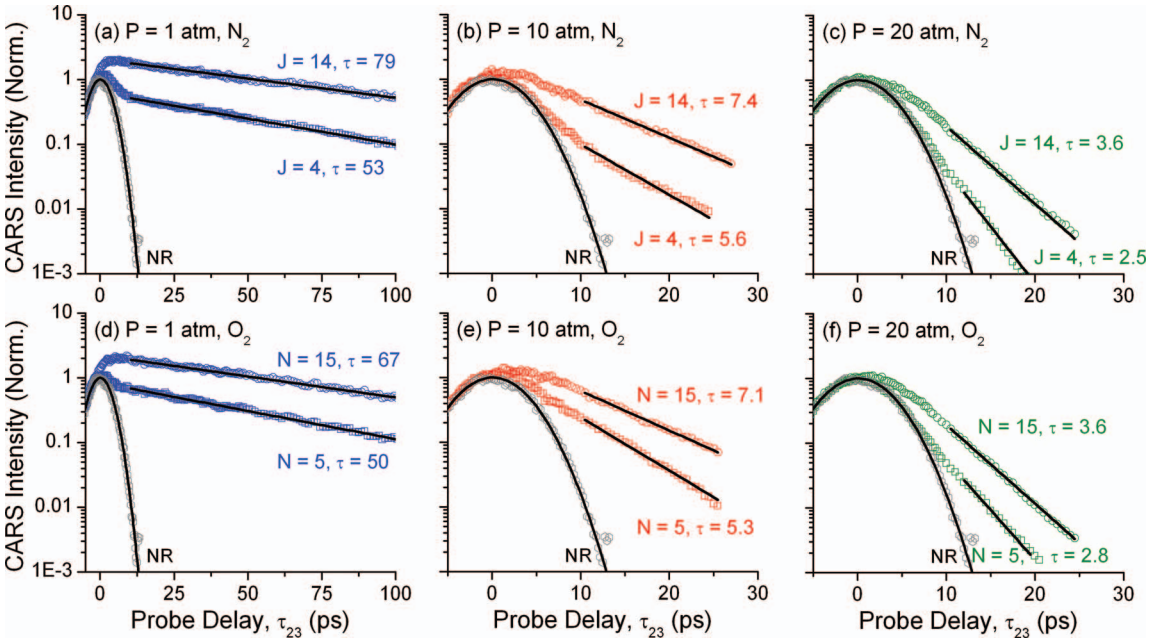

FIG. 1. Spectrally resolved hybrid fs/ps RCARS signals from $J = 4$ and 14 for N_2 at (a) 1 atm, (b) 10 atm, and (c) 20 atm and $N = 5$ and 15 for O_2 at (d) 1 atm, (e) 10 atm, and (f) 20 atm. Solid lines are exponential fits to signal decay.

at atmospheric pressure and was decreased at elevated pressure to avoid stimulated Raman pumping and interference from sustained molecular alignment. A 2-cm^{-1} full width at half maximum (FWHM), 8.1-ps probe pulse was formed in a 4-*f* pulse shaper by spectrally filtering the beam using a square slit. This bandwidth was sufficient to isolate individual transitions while minimizing the probe delay for nonresonant suppression. The slit was slightly rotated to produce a nearly Gaussian time-domain profile.[7] The three beams were focused in a BOXCARS phase-matching configuration using a 300-mm lens. The CARS beam was spatially filtered and then detected using a 0.303-m spectrometer with a 1200 line/mm grating and an electron-multiplied charge-coupled device camera. The gases were pressurized in a cylindrical stainless steel vessel equipped with a 1/16-inch diameter K-type thermocouple and digital pressure gauge (0–500 ±1.25 psi).

A theoretical description of the hybrid fs/ps RCARS process is given in Refs. 7, 8, and 13. Of particular interest here is the treatment of the molecular response function. For pure rotational transitions ($\Delta v = 0$), a phenomenological function is given as the summation of all active O-branch ($\Delta J = -2$) and S-branch transitions ($\Delta J = +2$) from state m to n

$$R(t) = \sum I_{n,m}(T)\, e^{-i\omega_{n,m}t - \Gamma_{n,m}t}, \tag{1}$$

where $I_{n,m}$ is the intensity of each rotational Raman transition as a function of temperature[7] and $\omega_{n,m}$ (s^{-1}) is the frequency of each transition. The linewidth, $\Gamma_{n,m}$ (s^{-1}), is related to the S-branch spectral linewidth (m^{-1}, FWHM) and decay constant, $\tau_{\mathrm{CARS},J+2,J}$ (s)

$$\Gamma_{J+2,J}|_t = 2\pi c \Gamma_{J+2,J}|_\omega = (\tau_{\mathrm{CARS},J+2,J})^{-1}, \tag{2}$$

where c is the speed of light (m/s).[5] The linewidth represents a single-exponential decay of the molecular response in time primarily due to inelastic molecular collisions.[2,14] The modified exponential gap (MEG) model is frequently employed to calculate the transition dependence (initial state m) of the collisional linewidth assuming a linear dependence on pressure.[14] In this work, comparisons are made with the MEG model using parameters for self-broadened N_2 and O_2 from Seeger *et al.*[11] and the rotational approximation of Martinsson *et al.*[15]

For simple linear molecules such as N_2, the rotational levels are well known and the rotational transitions are indicated by the total angular momentum, J, of the initial state. For O_2, the ground state exhibits a nuclear spin of zero and an electronic spin, S, of one which leads to a splitting of the rotational states into triplets.[16,17] In this case, the rotational transitions are given as a function of the rotational quantum number, N, of the initial state while the splitting occurs due to the N–S coupling with the total angular momentum given by $J = (N - 1, N, N + 1)$.[16]

Rotationally resolved RCARS signals of N_2 (298 K) and O_2 (295 K) are shown as a function of probe delay in Fig. 1 for pressures of 1, 10, and 20 atm. Three independent scans for each pressure were performed over a one week period to verify the repeatability. Only the $J = 4$ and 14 transitions for N_2 and $N = 5$ and 15 transitions for O_2 are shown for simplicity. The RCARS signals are compared to the normalized and spectrally integrated nonresonant background from argon to show the relative rates of decay. The time constant of each rotational transition was measured by fitting a single exponential function to the decay of the RCARS signal spectrally integrated over each individual transition, and the spectral linewidth was computed using Eq. (2). For most conditions, the fitting process was initiated after a probe delay of 10.5 ps when the nonresonant background dropped by 10^2, as shown in Fig. 1. At a fixed probe delay, however, the relative influence of the nonresonant background increased at higher

Author complimentary copy. Redistribution subject to AIP license or copyright, see http://jcp.aip.org/jcp/copyright.jsp

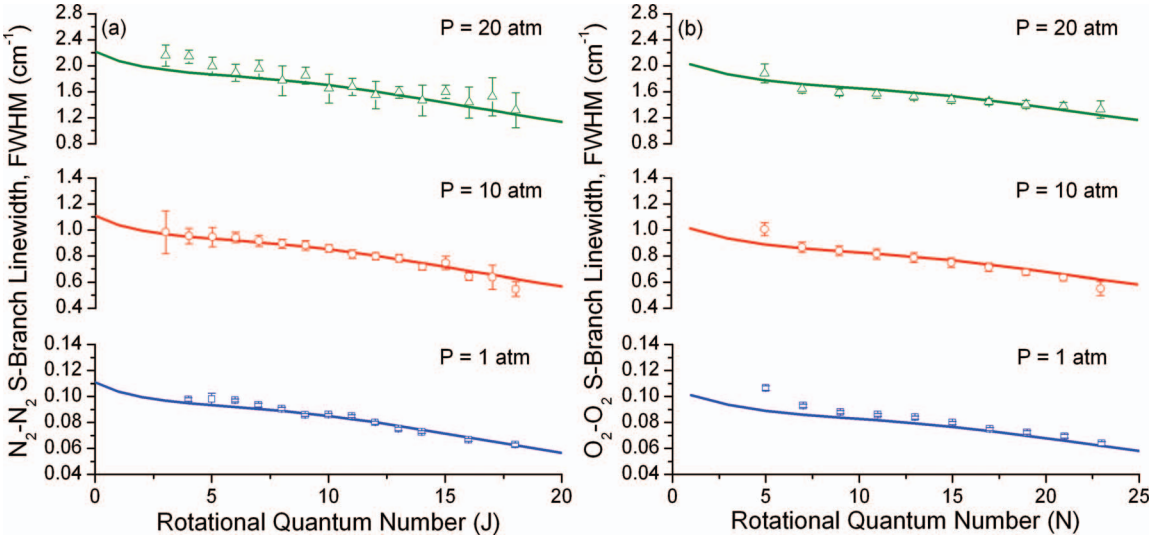

FIG. 2. Measured (a) N_2 and (b) O_2 self-broadened linewidths as a function of initial rotational state at pressures of 1, 10, and 20 atm. Solid lines are MEG linewidths using S-branch approximation. Bars represent calculated uncertainty.

pressure because the resonant signal was sensitive to collisions. To offset this effect, the fitting process for rotational transitions with the lowest signal levels was initiated at longer delays ($\geq$12 ps) to allow the nonresonant background to decay even further. This ensured that the signal-to-nonresonant ratio in the spectral band of each transition, estimated from the nonresonant susceptibilities of Ar, N_2, and O_2, was always 10^2 or higher.

The measured self-broadened S-branch linewidths are shown in Fig. 2 at pressures of 1, 10, and 20 atm and tabulated for pressures of 1, 2.5, 5, 10, 15, and 20 atm in Tables I and II. The uncertainty was calculated from the 95% confidence interval of the average fit with an additional systematic experimental uncertainty ($\sim$2%) combined in quadrature. The 95% confidence interval of the average data is comparable to the standard deviation from the three individual datasets. Generally, the S-branch linewidths were measured with 1%–2% uncertainty at 1 atm, which represents an improvement over previous frequency-domain measurements under similar conditions.[14,16] At the highest pressure of 20 atm, the decay rate constant is as small as 2.5 ps, leading to higher uncertainties for low and high rotational transitions of N_2 and O_2 and odd transitions of N_2.

The solid lines in Fig. 2 represent self-broadened linewidths for N_2 and O_2 computed using the MEG model Q-branch linewidths derived from frequency-domain measurements with the S-branch approximation.[11,15] The computed linewidths agree well with the current data for N_2 but deviate at low rotational levels as found in previous time-domain[4,7] and frequency-domain[18] measurements at 1 atm. This shift is due to re-orientation of the molecular axis after collisions, which does not contribute to Q-branch linewidths from which the MEG model was derived.[12]

The O_2 measured linewidths for high rotational numbers are in agreement with the MEG model at 1 atm and with previous S-branch measurements using spontaneous Raman

TABLE I. Experimental N_2 self-broadened linewidths, FWHM (cm^{-1}).

J	1 atm	2.5 atm	5 atm	10 atm	15 atm	20 atm
3		0.266 ± 0.020		0.984 ± 0.165		2.158 ± 0.162
4	0.098 ± 0.001	0.259 ± 0.016	0.505 ± 0.023	0.954 ± 0.060	1.518 ± 0.186	2.140 ± 0.099
5	0.098 ± 0.004	0.262 ± 0.017	0.490 ± 0.025	0.946 ± 0.074	1.505 ± 0.233	1.993 ± 0.141
6	0.097 ± 0.001	0.256 ± 0.017	0.468 ± 0.017	0.943 ± 0.040	1.397 ± 0.174	1.891 ± 0.129
7	0.093 ± 0.001	0.236 ± 0.015	0.456 ± 0.019	0.917 ± 0.043	1.357 ± 0.162	1.956 ± 0.134
8	0.090 ± 0.001	0.233 ± 0.015	0.441 ± 0.015	0.895 ± 0.034	1.335 ± 0.157	1.772 ± 0.230
9	0.086 ± 0.001	0.226 ± 0.015	0.428 ± 0.015	0.882 ± 0.037	1.278 ± 0.170	1.850 ± 0.129
10	0.086 ± 0.001	0.229 ± 0.014	0.430 ± 0.015	0.858 ± 0.029	1.252 ± 0.152	1.649 ± 0.222
11	0.085 ± 0.001	0.221 ± 0.014	0.398 ± 0.015	0.814 ± 0.033	1.192 ± 0.175	1.678 ± 0.130
12	0.080 ± 0.001	0.203 ± 0.013	0.383 ± 0.014	0.798 ± 0.027	1.162 ± 0.149	1.553 ± 0.214
13	0.075 ± 0.001	0.199 ± 0.013	0.362 ± 0.020	0.783 ± 0.030	1.088 ± 0.178	1.594 ± 0.090
14	0.073 ± 0.001	0.194 ± 0.013	0.358 ± 0.014	0.717 ± 0.026	1.051 ± 0.150	1.466 ± 0.235
15		0.191 ± 0.015	0.314 ± 0.018	0.747 ± 0.051	0.926 ± 0.172	1.597 ± 0.105
16	0.067 ± 0.001	0.173 ± 0.012	0.308 ± 0.016	0.643 ± 0.028	0.931 ± 0.145	1.435 ± 0.239
17			0.265 ± 0.050	0.637 ± 0.092	0.790 ± 0.186	1.522 ± 0.294
18	0.063 ± 0.001	0.158 ± 0.019	0.246 ± 0.025	0.548 ± 0.055	0.815 ± 0.147	1.316 ± 0.272

Author complimentary copy. Redistribution subject to AIP license or copyright, see http://jcp.aip.org/jcp/copyright.jsp

TABLE II. Experimental O_2 self-broadened linewidths, FWHM (cm^{-1}).

N	1 atm	2.5 atm	5 atm	10 atm	15 atm	20 atm
5	0.107 ± 0.002	0.244 ± 0.015	0.459 ± 0.017	1.006 ± 0.051	1.329 ± 0.039	1.881 ± 0.145
7	0.093 ± 0.001	0.221 ± 0.013	0.434 ± 0.016	0.866 ± 0.040	1.282 ± 0.036	1.646 ± 0.070
9	0.088 ± 0.001	0.212 ± 0.013	0.420 ± 0.014	0.840 ± 0.036	1.243 ± 0.034	1.588 ± 0.056
11	0.086 ± 0.001	0.213 ± 0.013	0.409 ± 0.015	0.815 ± 0.039	1.200 ± 0.039	1.569 ± 0.067
13	0.084 ± 0.001	0.209 ± 0.013	0.398 ± 0.015	0.787 ± 0.036	1.155 ± 0.039	1.523 ± 0.050
15	0.080 ± 0.001	0.196 ± 0.012	0.374 ± 0.015	0.749 ± 0.035	1.114 ± 0.039	1.485 ± 0.061
17	0.075 ± 0.001	0.186 ± 0.012	0.353 ± 0.015	0.714 ± 0.032	1.034 ± 0.042	1.448 ± 0.051
19	0.072 ± 0.001	0.183 ± 0.012	0.333 ± 0.017	0.676 ± 0.025	0.968 ± 0.040	1.406 ± 0.062
21	0.069 ± 0.001	0.168 ± 0.012	0.310 ± 0.023	0.635 ± 0.027	0.927 ± 0.068	1.380 ± 0.056
23	0.064 ± 0.002	0.163 ± 0.016	0.261 ± 0.055	0.552 ± 0.054	0.807 ± 0.144	1.329 ± 0.134

scattering.[16] The linewidths of the low rotational states are influenced by the triplet ground state of the O_2 molecule, which exhibits three transitions (S_-, S_0, and S_+) separated by ~1.99 cm^{-1}.[16] Because the triplet is spectrally overlapped by the probe pulse, this separation results in a temporal oscillation of the RCARS signal, as shown in Fig. 3 for $N = 1$ and 3 at 1 atm. A cosine function is used to fit the oscillation with resulting periods of 16.8 ps and 16.9 ps for $N = 1$ and 3, respectively. These represent separations of 1.98 cm^{-1} and 1.97 cm^{-1}, which are within 1% of theoretical and experimental values.[16] While the intensity of the triplets are of the same order for $N = 1$, they are negligible for $N > 5$.[16] At elevated pressure, the CARS signal decays significantly within the first period of the triplet oscillation; thus, the oscillation cannot be resolved, and the measured linewidths may be larger than expected due to interference of the triplet oscillation. For this reason we have not reported linewidth data for $N = 1$ and 3 in this work.

In summary, hybrid fs/ps RCARS was used to measure the collisional decay rates and individual S-branch transition linewidths of N_2 and O_2 from 1–20 atm. Excellent sensitivity to transition-resolved signal decay was achieved at high pressures where the rate constants are as low as 2.5 ps. Agreement was found with previous N_2 and O_2 S-branch measurements available at low pressure which indicate a small positive offset from the MEG model. This relationship was confirmed at high pressures. The accuracy for low J levels of N_2 at higher pressure was bounded by a combination of nonresonant background, small decay rate constants, and low spectral intensity. In the case of O_2, oscillations in the time decay due to interference of the triplet ground state limited the accuracy of linewidth measurements for low rotational states.

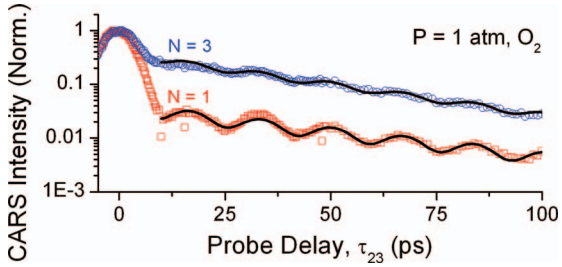

FIG. 3. Decay of $N = 1$ and 3 rotational lines of O_2. Solid lines show measured oscillations due to triplet ground state with periods of 16.8 ps and 16.9 ps, respectively.

Funding was provided by the National Science Foundation (CBET-1056006, Dr. A. Atreya, Program Official) and the Air Force Office of Scientific Research (Dr. R. Parra and Dr. C. Li, Program Managers). J. Miller was supported by the National Science Foundation Graduate Fellowship Program. The authors also thank C. Dedic, M. Johnson, and B. Halls of Iowa State University.

[1] S. Roy, J. R. Gord, and A. K. Patnaik, Prog. Energy Combust. Sci. **36**, 280 (2010).
[2] G. Knopp, P. Beaud, P. Radi, M. Tulej, B. Bougie, D. Cannavo, and T. Gerber, J. Raman Spectrosc. **33**, 861 (2002).
[3] M. Motzkus, T. Lang, H. M. Frey, and P. Beaud, J. Chem. Phys. **115**, 5418 (2001).
[4] C. J. Kliewer, Y. Gao, T. Seeger, J. Kiefer, B. D. Patterson, and T. B. Settersten, Proc. Combust. Inst. **33**, 831 (2011).
[5] W. D. Kulatilaka, P. S. Hsu, H. U. Stauffer, J. R. Gord, and S. Roy, Appl. Phys. Lett. **97**, 081112 (2010).
[6] T. Seeger, J. Kiefer, A. Leipertz, B. D. Patterson, C. J. Kliewer, and T. B. Settersten, Opt. Lett. **34**, 3755 (2009).
[7] J. D. Miller, S. Roy, M. N. Slipchenko, J. R. Gord, and T. R. Meyer, Opt. Express **19**, 15627 (2011).
[8] J. D. Miller, M. N. Slipchenko, T. R. Meyer, H. U. Stauffer, and J. R. Gord, Opt. Lett. **35**, 2430 (2010).
[9] S. Roy, P. Wrzesinski, D. Pestov, T. Gunaratne, M. Dantus, and J. R. Gord, Appl. Phys. Lett. **95**, 074102 (2009).
[10] J. D. Miller, M. N. Slipchenko, and T. R. Meyer, Opt. Express **19**, 13326 (2011).
[11] T. Seeger, F. Beyrau, A. Brauer, and A. Leipertz, J. Raman Spectrosc. **34**, 932 (2003).
[12] M. Afzelius, P. E. Bengtsson, J. Bood, J. Bonamy, F. Chaussard, H. Berger, and T. Dreier, Appl. Phys. B **75**, 771 (2002).
[13] B. D. Prince, A. Chakraborty, B. M. Prince, and H. U. Stauffer, J. Chem. Phys. **125**, 044502 (2006).
[14] L. A. Rahn and R. E. Palmer, J. Opt. Soc. Am. B **3**, 1164 (1986).
[15] L. Martinsson, P. E. Bengtsson, M. Alden, S. Kroll, and J. Bonamy, J. Chem. Phys. **99**, 2466 (1993).
[16] M. Berard, P. Lallemand, J. P. Cebe, and M. Giraud, J. Chem. Phys. **78**, 672 (1983).
[17] G. Millot, R. Saintloup, J. Santos, R. Chaux, H. Berger, and J. Bonamy, J. Chem. Phys. **96**, 961 (1992).
[18] G. Fanjoux, G. Millot, and B. Lavorel, J. Raman Spectrosc. **27**, 475 (1996).

Author complimentary copy. Redistribution subject to AIP license or copyright, see http://jcp.aip.org/jcp/copyright.jsp